Krumm, Sabine; Kivisaari, Sasa L.; Probst, Alphonse; Monsch, Andreas U.; Reinhardt, Julia; Ulmer, Stephan; Stippich, Christoph; Kressig, Reto W.; Taylor, Kirsten I.

Cortical thinning of parahippocampal subregions in very early Alzheimer's disease

Published in:
Neurobiology of Aging

DOI:
10.1016/j.neurobiolaging.2015.11.001

Published: 01/01/2016

Document Version
Publisher's PDF, also known as Version of record

Neurobiology of Aging 38 (2016) 188–196

Contents lists available at ScienceDirect

Neurobiology of Aging

journal homepage: www.elsevier.com/locate/neuaging

Cortical thinning of parahippocampal subregions in very early Alzheimer's disease

Sabine Krumm [a,b,*], Sasa L. Kivisaari [c], Alphonse Probst [a,d], Andreas U. Monsch [a,b], Julia Reinhardt [e], Stephan Ulmer [f,g], Christoph Stippich [b,e], Reto W. Kressig [a,h], Kirsten I. Taylor [a,b,i,1]

[a] Memory Clinic, University Center for Medicine of Aging Basel, Felix-Platter Hospital, Basel, Switzerland
[b] Faculty of Psychology, University of Basel, Basel, Switzerland
[c] Department of Neuroscience and Biomedical Engineering, Aalto University School of Science, Aalto, Finland
[d] Department of Neuropathology, Institute of Pathology, University Hospital Basel, Basel, Switzerland
[e] Department of Radiology, Division of Diagnostic and Interventional Neuroradiology University Hospital Basel, Basel, Switzerland
[f] Institute of Neuroradiology, University Hospital Schleswig-Holstein, Kiel, Germany
[g] Medical Radiological Institute (MRI), Zurich, Switzerland
[h] Faculty of Medicine, University of Basel, Basel, Switzerland
[i] Centre for Speech, Language and the Brain, Department of Experimental Psychology, University of Cambridge, Cambridge, UK

ARTICLE INFO

Article history:
Received 9 February 2015
Received in revised form 2 November 2015
Accepted 3 November 2015
Available online 10 November 2015

Keywords:
Perirhinal cortex
Entorhinal cortex
Parahippocampal cortex
Amnestic mild cognitive impairment
Atrophy
Structural MRI

ABSTRACT

The stereotypical pattern of neurofibrillary tangle spreading in the earliest stages of typical Alzheimer's dementia (AD) predicts that medial perirhinal cortex (mPRC) atrophy precedes entorhinal cortex (ERC) atrophy, whereas the status of the parahippocampal cortex (PHC) remains unclear. Atrophy studies have focused on more advanced rather than early AD patients, and usually segment the entire PRC as opposed to the mPRC versus lateral PRC (lPRC). The present study therefore determined the extent of ERC, mPRC, lPRC, and PHC atrophy in very early AD (mean Mini-Mental State Examination score = 26) patients and its presumed prodrome amnestic mild cognitive impairment (mean Mini-Mental State Examination score = 28) compared to demographically matched controls. PHG structures were manually segmented (blinded rater) and cortical thicknesses extracted. ERC and mPRC were similarly atrophied in both patient groups. The lPRC was atrophied in the AD group only. Thus, atrophic changes in very early AD broadly map onto the pattern of neurofibrillary tangle spreading and suggest that mPRC, ERC, and lPRC, but not PHC-associated functional impairments, characterize very early-stage AD.

1. Introduction

The early stages of Alzheimer's dementia (AD) are associated with atrophy of the parahippocampal gyrus (PHG, i.e., entorhinal cortex [ERC], perirhinal cortex [PRC] and parahippocampal cortex [PHC]) of the medial temporal lobe (MTL). In typical AD, neurofibrillary tau pathology begins in the transentorhinal cortex (i.e., medial PRC [mPRC]), from where it spreads to the ERC (transentorhinal stages) and to the hippocampal subfields (limbic stages) before spreading into the lateral PRC (lPRC) and isocortical structures (Braak and Braak, 1991; Braak and Del Tredici, 2006; Kordower et al., 2001; Taylor and Probst, 2008). Most investigations of atrophy in AD or its putative prodrome amnestic mild cognitive impairment (aMCI) focus on ERC and hippocampal atrophy, but rarely on that of the PRC, in particular its medial versus lateral aspects (e.g., Du et al., 2001). Also, it is unclear to what extent the PHC is affected in the earliest stages of AD. Finally, it remains unclear whether the brunt of PHG thinning is concentrated in specific anterior-to-posterior levels and, thus, which corresponding coronal levels are optimally clinically informative for distinguishing between healthy normal controls (NCs) and very early AD patients. The present study addresses these questions by manually segmenting the key PHG structures on high-resolution magnetic resonance imaging (MRI) scans according to a

* Corresponding author at: Felix-Platter Hospital, University Center for Medicine of Aging Basel, Memory Clinic, Schanzenstrasse 55, CH-4031 Basel, Switzerland. Tel.: +41 (0)61 265 94 25; fax: +41 (0)61 265 37 88.
E-mail address: sabine.krumm@fps-basel.ch (S. Krumm).
[1] Present address: Biomarkers and Clinical Imaging, Neuroscience, Ophthalmology, and Rare Diseases (NORD), Roche Pharma Research and Early Development, Roche Innovation Center Basel, F. Hoffmann-La Roche Ltd, Grenzacherstrasse 124, CH-4070 Basel, Switzerland.

http://dx.doi.org/10.1016/j.neurobiolaging.2015.11.001

cytoarchitectonic-, chemoarchitectonic-, and connectivity-based protocol (Insausti et al., 1998; Kivisaari et al., 2013b; Taylor and Probst, 2008) in a large group of healthy control subjects and very early AD patients.

The progressive accumulation of neurofibrillary tangles (NFTs) is assumed to be causally related to cortical atrophy in AD (Ball, 1978; Gómez-Isla et al., 1997). Pyramidal cells in the mPRC are the first cortical neurons to be affected by NFTs (stage I; Braak and Braak, 1991, 1995; Kordower et al., 2001). We note that the mPRC corresponds to Braak and Braak (1991) "transentorhinal cortex" (Taylor and Probst, 2008). Next, cells in layer II of the ERC are affected before pathology spreads to the hippocampal formation (stage II) and into layer IV of the ERC (stage III) (Braak and Del Tredici, 2006). The lPRC is affected in stage III (Braak and Braak, 1991; Braak and Del Tredici, 2006; Van Hoesen et al., 2000). If atrophy mainly results from tau pathology, this progression of pathology predicts that cortical thinning of the mPRC precedes that of the lateral ERC. However, this pattern may not be apparent on structural MRI, since the involvement of a single cortical layer (e.g., mPRC stages I, II) may not cause sufficient cortical thinning for its detection on structural MRI scans. That is, ERC atrophy may be visible on MRI before mPRC atrophy, because 2 independent cortical layers of the ERC (i.e., layers II and IV) are affected early in the disease process compared to a single mPRC layer. Moreover, it is unclear whether the PHC is affected by the pathological tau accumulation in the earliest stages of AD. This is a critical point, since early PHC atrophy could explain some of the cognitive (e.g., visuospatial: Epstein and Kanwisher, 1998) impairments associated with early AD.

MRI-based studies of regional PHG integrity in mild-to-moderate AD patients consistently report atrophy of these structures. Juottonen et al. (1998) compared the ERC, entire PRC, and temporopolar cortex volumes of 30 AD patients (Mini-Mental State Examination [MMSE; Folstein et al., 1975] range 14–28) with 32 NC participants. They found that each region was significantly atrophied in AD patients, with the ERC significantly more severely affected than the entire PRC. Similarly, Teipel et al. (2006) reported comparable extents of atrophy when analyzing the volumes of the entire PRC, PHC, and ERC of AD patients ($n = 34$; MMSE scores ≥ 10) to NCs ($n = 22$). Measures of cortical thickness may provide a more accurate measure of atrophy than 3-dimensional volumes, especially in anatomically highly variable regions such as the PRC, where volumetric measurements are confounded by the size of this structure which varies widely between individuals according to the depth and number of collateral sulci (CS; Insausti et al., 1998). Using mean cortical thickness measurements, Lerch et al. (2005) demonstrated severe cortical thinning of the entire PHG in 19 AD patients (MMSE range, 10–29) compared to 17 NCs, with a significant group difference in the anterior portion of the left ERC, which was the only cytoarchitectonic field that was individually segmented. Dickerson et al. (2009) segmented each PHG subfield in 29 AD patients (MMSE range, 16–28) and found significant cortical thinning of the ERC, mPRC (estimated by the medial bank of the collateral sulcus), and PHC compared to 47 NC participants. Taken together, these studies demonstrate significant and comparable extents of atrophy in the ERC, PRC, and PHC in the mild-to-moderate stages of AD.

The comparable degree of PHG atrophy reported in the aforementioned studies does not at first blush map onto the progression of NFT pathology as described by Braak and Braak (1995). However, the AD patients investigated were either in mild-to-moderate stages of the disease, or the samples were highly variable with respect to disease stage (MMSE scores range from 10 to 29). Thus, neurofibrillary pathology was presumably more dense and widespread compared to patients in the early stages of the disease. Therefore, very early AD patients who are expected to be in early stages of NFT pathology should be examined (Geddes et al., 1997; Nelson et al., 2012). Second, it is essential to segment the mPRC from the lPRC, as cortical NFT begins in the mPRC (stage I), whereas the lPRC is only affected by NFT in stage IV. The anatomic borders of the mPRC corresponding to Braak and Braak's "transentorhinal region" were described by Taylor and Probst (2008) and subsequently integrated into an MTL segmentation protocol (Kivisaari et al., 2013b) incorporating aspects of the Insausti et al. (1998) criteria. Given the high anatomic variability of the CS, which defines mPRC and lPRC boundaries, it is necessary to segment these structures manually to achieve anatomic precision (Hanke, 1997; Pruessner et al., 2002).

The purpose of the present study was to adopt the approach described previously to determine the location and extent of cortical thinning in the ERC, mPRC, lPRC, and PHC in 2 groups of patients with very early AD, that is, a group of aMCI patients presumed to be in the prodromal phases of AD (Petersen et al., 2006), and a group of mildly affected AD patients. All regions of interest (ROIs) were manually segmented by an investigator blinded to diagnosis (Sabine Krumm) using an anatomical protocol recapitulated here (Kivisaari et al., 2013b). Specifically, we aimed to determine whether, in the very early stages of AD, (1) the mPRC and/or ERC is significantly atrophied (1 vs. 2 layers) and (2) PHC thinning is apparent. The first question tests the hypothesis that cortical thinning maps onto the pattern of neurofibrillary pathology, and the second question addresses the unknown status of the PHC in the earliest stages of AD. Both issues are highly clinically relevant as they advise clinicians of the anatomic structures to focus on during the diagnostic process and indicate which corresponding cognitive impairments are expected in the early stages of AD (see e.g., Kivisaari et al., 2012). Finally, we asked whether (3) cortical thinning is maximized in specific anterior-to-posterior coronal levels which would reflect the optimal slices on which to clinically detect very early AD.

2. Methods

2.1. Participants

Data from 121 native Swiss-German or German-speaking adults were included in the present study: 64 healthy control participants (NC) and 57 individuals with very early AD (see the following paragraph). The healthy control participants had undergone a thorough medical screening and neuropsychological testing to ensure that they were cognitively (i.e., neurologically and psychiatrically) healthy. Specifically, exclusion criteria included severe auditory, visual or speech deficits; severe sensory or motor deficits; severe systemic disease; continuous mild-to-intense pain; diseases with severe or probable impact on the central nervous system (e.g., neurologic disorders including cerebral-vascular disease, generalized atherosclerosis, and psychiatric problems); and intake of potent psychoactive substances except mild tranquilizers. In addition, all NCs received normal scores on the MMSE (Folstein et al., 1975), California Verbal Learning Task (Delis et al., 1987), Clock Drawing Test (Critchley, 1953), and short version of the Boston Naming Test (Kaplan et al., 1983).

Thirty-four participants (16 male, 18 female) were diagnosed with AD according to NINCDS-ADRDA and DSM-IV criteria (American Psychichiatric Association, 1994) and 23 patients (11 male, 12 female) with mild neurocognitive disorder because of AD according to DSM-IV and Winblad et al. (2004) criteria (aMCI; single-, or multi-domain). All patients had been recruited from the Memory Clinic, University Center for Medicine of Aging in Basel, Switzerland, where they had received neuropsychological testing, MRI scanning, and medical and neurological examinations including blood analyses.

As many NC participants as possible were demographically matched to the aMCI group and AD patients with regard to age, gender, and education (all p-values > 0.3; see Table 1). As expected, mean MMSE scores of the aMCI and the AD groups significantly differed from their respective control groups (NC vs. aMCI: $F(1,67) = 8.55$, $p < 0.01$; NC vs. AD: $F(1,63) = 47.19$, $p < 0.001$). Critically, the mean MMSE scores of both patients groups indicate that they were mildly affected.

2.2. MRI measures

2.2.1. MRI acquisition

All participants received MRI scanning conducted on a 3-T head scanner (MAGNETOM Verio, Siemens) at the University Hospital Basel (T1-weighted 3D magnetization-prepared rapid acquisition gradient echo; inversion time = 1000 ms; repetition time = 2000 ms; echo time = 3.75 ms; flip angle = 8°; field of view = 256 × 256; acquisition matrix = 256 × 256 mm; voxel size = 1 mm isotropic).

2.2.2. Preprocessing of structural MR images

Preprocessing of MRI scans was conducted using FreeSurfer (Massachusetts General Hospital, Boston, MA; http://surfer.nmr.mgh.harvard.edu; Dale et al., 1999; Fischl and Dale, 2000). Magnetization-prepared rapid acquisition gradient echo volumes were semiautomatically segmented into gray and white matter and the pial and gray/white matter surfaces were formed (Dale et al., 1999). Tissue next to the anteromedial temporal lobe was removed by hand because it interfered with the cortical surface reconstructions. The cortical thickness is defined as the distance between corresponding vertices on the gray/white matter and pial surfaces. The total intracranial volume (TIV; gray matter + white matter + CSF volumes) per participant was estimated using SPM8 (Wellcome Institute of Cognitive Neurology) implemented in Matlab 2010 (Mathworks Inc., Sherborn, MA, USA).

2.2.3. Regions of interest

To our knowledge, no available software accurately and automatically segments the mPRC and lPRC on MRI images. However, the creation of labels for these regions is necessary to extract cortical thickness data. MTL ROIs were therefore manually drawn by a blinded rater (Sabine Krumm) on coronal slices of the native space cortical surface reconstructions generated by FreeSurfer according to anatomic landmarks described in Kivisaari et al. (2013b) which was based primarily on Insausti et al. (1998). We note that the major deviation between the Insausti et al. (1998) and Kivisaari et al. (2013b) protocols is the latter's inclusion of landmarks to segment the mPRC and lPRC based on Taylor and Probst (2008). Left and right hemispheric ROIs were drawn for the mPRC, lPRC, ERC, and PHC. The mPRC corresponds to the transentorhinal region, considered as an area of transition between ERC and PRC (Braak and Braak, 1985; Taylor and Probst, 2008). For the purposes of the present study, only portions of the PRC lateral to the ERC were segmented, that is, the most anterior and posterior aspects of the PRC, which wrap medially around the most anterior and posterior part of the ERC, were not segmented because to our knowledge no cytoarchitectonic data exist to delineate the PRC subregions here (Taylor and Probst, 2008). The detailed manual segmentation protocol is described in Table 2 [structured in the style of Pruessner et al., (2002)]. We note that the proportions of shallow, normal, and deep CS were comparable in the aMCI and the respective control group ($\chi^2 = 2.450$, $p = 0.294$), as were proportions of single versus bifurcated CS in both patient groups (aMCI vs. NC: $\chi^2 = 0.579$, $p = 0.447$; AD vs. NC: $\chi^2 = 0$, $p = 1$) and shallow, normal, and deep bifurcated sulci (aMCI vs. NC: $\chi^2 = 3.36$, $p = 0.186$; AD vs. NC: $\chi^2 = 0.087$, $p = 0.768$). Alone the proportion of shallow, normal, and deep CS significantly differed between the AD and their NC group (AD vs. NC: $\chi^2 = 16.804$, $p < 0.001$) as a consequence of the more frequent occurrence of shallow CS in the AD group (AD vs. NC: 62% vs. 36%), consistent with their atrophy and thus sulcal flattening (Im et al., 2008). However, we note that PRC cortical thickness values are less susceptible to variations in CS depth compared to "volumetric" measures (see the previously mentioned paragraphs).

2.2.4. Cortical thickness estimates

Three-dimensional measurements of atrophy in PHG regions and especially the PRC, such as volumetric measures, depend on the number and depth of the CS (i.e., deeper CS are associated with more voluminous PRCs). To compare atrophy across ROIs while controlling for intraindividual differences in the size of the PRCs, we used a measure that is independent of volume (i.e., the depth of the collateral sulcus), namely the cortical thickness of each manually segmented ROI. Mean cortical thickness values for each ROI were obtained using FreeSurfer (Massachusetts General Hospital, Boston, MA; http://surfer.nmr.mgh.harvard.edu; Dale et al., 1999; Fischl and Dale, 2000), and individual cortical thickness values for each vertex were extracted using Matlab 2010 (Mathworks Inc., Sherborn, MA; USA). By default, FreeSurfer sets the cortical thickness maximum to 5 mm because a former study demonstrated that this upper limit included the large majority of cortical thickness estimates (Fischl and Dale, 2000). However, 2.4% of our thickness values exceeded the 5 mm maximum, resulting in a non-normal distribution. Therefore, we changed this limit to 10 mm and visually inspected the location of each vertex exceeding 5 mm. Two of 9384 vertices were not lying within our ROIs and were therefore excluded; the remaining vertices were included in the subsequent analyses. The right-anterior-superior coordinates were converted into Montral Neurological Institute (MNI) coordinates in FreeSurfer. Mean patient cortical thickness values were transformed into standard (z-) scores for graphic visualization according to the following formulae: ([mean patient cortical thickness value]−[corresponding mean NC cortical thickness])/(corresponding NC standard deviation of mean cortical thickness). Three-dimensional graphical depictions of these vertex-wise mean cortical thickness z-scores representing NC and patient differences in cortical thickness over the cortical surface were plotted in Matlab 2010.

Table 1
Demographic characteristics and MMSE scores for the demographically matched NC and aMCI and AD samples

Variable	NC versus aMCI		NC versus early AD	
	NC (n = 46)	aMCI (n = 23)	NC (n = 31)	Early AD (n = 34)
	Mean ± SD	Mean ± SD	Mean ± SD	Mean ± SD
Age	74.78 ± 7.09	76.08 ± 8.26	78.10 ± 5.58	78.89 ± 5.24
Gender[a]	1.41 ± 0.50	1.52 ± 0.51	1.42 ± 0.50	1.53 ± 0.51
Education	13.41 ± 3.10	14.00 ± 3.66	12.55 ± 2.46	12.24 ± 3.04
MMSE score	29.26 ± 1.10	28.22 ± 1.86**	29.19 ± 1.05	26.32 ± 2.09**

Key: AD, Alzheimer's dementia; aMCI, amnestic mild cognitive impairment; MMSE, Mini-Mental State Examination; NC, normal controls; SD, standard deviation.
[a] ♂ = 1; ♀ = 2; significant difference compared to respective NC group at $^{**}p < 0.01$ (unpaired, 2-tailed t tests).

2.3. Statistical analyses

Cortical thickness estimates used in the statistical analyses were normalized for head size (TIV; [(cortical thickness)/(TIV)] × 100) and retransformed into metric values (mm) for tabular reporting to facilitate interpretation. To determine which demographic variables and whether hemisphere should be included as covariates in the statistical analyses of group differences, we performed a

Table 2
Segmentation protocol for the mPRC, lPRC, ERC, and PHC (CS) based on structural MRI scans of 1 mm^3 resolution

Structure	Anterior border	Posterior border	Medial border	Lateral border	Comments
ERC	2 mm posterior to the first anterior slice where the white matter of the limen insulae is visible.	1 mm posterior to the last slice still containing the apex of the intralimbic gyrus.	Midpoint of the gyrus ambiens. If not visible, the shoulder of the superomedial bank of parahippocampal gyrus.	Shoulder of the medial bank of the CS.	A CS is typically visibly at the level of the anterior border. However, in the sections where the CS begins but is not yet fully formed, the border is estimated from more posterior slices with an obvious CS.
Medial PRC	Same coronal level as the anterior border of the ERC, i.e., 2 mm posterior to the first anterior slice where the white matter of the limen insulae is visible.	1 mm posterior to the last slice still containing the apex of the intralimbic gyrus.	Shoulder of the medial bank of the CS.	Small or regular CS (≤1.5 cm): fundus of the CS. Deep CS (>1.5 cm): midpoint between shoulder of medial bank of CS and midpoint of lateral bank of CS.	If the CS is bifurcated, the criteria apply to the most medial sulcus.
Lateral PRC	Same coronal level as the anterior border of the ERC, i.e., 2 mm posterior to the first anterior slice where the white matter of the limen insulae is visible.	1 mm posterior to the last slice still containing the apex of the intralimbic gyrus.	Small or regular CS (≤1.5 cm): fundus of the CS. Deep CS (>1.5 cm): midpoint between shoulder of medial bank of CS and midpoint of lateral bank of CS.	Regular CS (1–1.5 cm): shoulder of lateral bank of CS. Shallow CS (<1 cm): midpoint of fusiform gyrus. Deep CS (>1.5 cm): midpoint between CS fundus and shoulder of its lateral bank.	If the CS is bifurcated, the criteria apply to the most medial sulcus.
PHC	4 mm posterior to the last slice containing the apex of the intralimbic gyrus.	First posterior slice where the pulvinar is no longer visible.	Medial apex of the parahippocampal gyrus, neighboring subiculum of the hippocampus.	Regular CS (1–1.5 cm): shoulder of lateral bank of CS. Shallow CS (<1 cm): midpoint of fusiform gyrus. Deep CS (>1.5 cm): midpoint between fundus and shoulder of lateral bank of CS.	The PHC is considered the posterior gyral continuation of the combined PRC and ERC.

This protocol segments the transentorhinal area of the PRC lateral to the ERC; therefore, the most anterior and posterior portions of the PRC wrapping around the ERC (e.g., 3–4 mm posterior to the last slice still containing the apex of the intralimbic gyrus) were not included in the mPRC and lPRC ROIs.
Key: CS, collateral sulcus; ERC, entorhinal cortex; lPRC, lateral perirhinal cortex; mPRC, medial perirhinal cortex; MRI, magnetic resonance imaging; PHC, parahippocampal cortex; ROI, region of interest.

univariate analysis of covariance (ANCOVA) using normalized mean cortical thickness values of the entire NC group (n = 64; mean age [±SD] = 72.97 [7.15], 40 male, 24 female; mean education [±SD] = 13.17 [3.05], mean MMSE score [±SD] = 29.19 [1.09]) as the dependent variable; the hemispheres and the 4 ROIs as independent variables; and sex, education, and age as covariates. Sex and education were significantly related to mean thickness values [female > male; $F(1, 501) = 72.454$, $p < 0.001$; $F(1, 501) = 5.908$, $p < 0.05$; no consistent education pattern] while age was not [$F(1, 501) = 7.5 \times 10^{-5}$, ns]. Hemisphere significantly interacted with ROI [$F(1, 501) = 2.727$, $p < 0.05$] although this difference did not survive Bonferroni correction. Based on these results, and previous reports of a significant association between age and gray matter thickness or volume (Scahill et al., 2002; Seo et al., 2011; Skullerud, 1984), all 3 demographic variables were included as covariates in all analyses of group differences, and cortical thickness estimates in each ROI were collapsed over the hemispheres. Post hoc 2-sided t tests were corrected according to the Hochberg GT2 procedure for unequal sample sizes. Significance levels were corrected for multiple comparisons according to Bonferroni. All statistical analyses were performed using SPSS 21.0 (IBM Corp Released 2012. IBM SPSS Statistics for Windows, version 21.0, Armonk, NY, USA).

3. Results

3.1. Regional parahippocampal gyrus thinning in aMCI and AD patients

Two-tailed, univariate ANCOVAs with sex, age, and education as covariates were performed to determine whether each PHG ROI was atrophied in the aMCI and AD groups relative to their corresponding NC sample. Significance was tested with Bonferroni-corrected p-values (i.e., $p = 0.05/8 = 0.00625$). With respect to the aMCI group, these revealed that the ERC and mPRC, but not the lPRC and PHC, were significantly atrophied in the aMCI group [ERC: $F(1,64) = 13.259$, $p < 0.00625$, mPRC: $F(1,64) = 10.587$, $p < 0.00625$, lPRC: $F(1,64) = 4.544$, $p > 0.00625$, PHC: $F(1,64) = 3.496$, $p = 0.066$]. A univariate ANCOVA with ERC versus mPRC ROI and diagnostic category revealed that these structures were atrophied to similar extents in the aMCI group [nonsigificant interaction; $F(1, 131) = 0.011$, $p = 0.916$].

The AD versus NC comparison revealed that the ERC, mPRC, and lPRC, but not the PHC, were significantly atrophied in the AD group [ERC: $F(1,60) = 52.650$, $p < 0.00625$, mPRC: $F(1,60) = 39.726$, $p < 0.00625$, lPRC: $F(1,60) = 8.243$, $p < 0.00625$, PHC: $F(1,60) = 4.769$, $p = 0.033 < 0.05$ i.e., did not survive Bonferroni correction of 0.00625]. Similar to the aMCI group, the extent of cortical thinning (relative to NCs) in the AD's ERC versus mPRC, as well as mPRC versus lPRC did not differ [no significant interaction of group and ROI: ERC vs. mPRC: $F(1, 123) = 0.038$, $p = 0.844$; mPRC versus lPRC: $F(1, 123) = 3.346$, $p = 0.070$]. However, atrophy in the ERC differed significantly from atrophy in the lPRC [$F(1, 123) = 4.229$, $p < 0.05$].

The mean cortical thickness values for each ROI per group are provided in Table 3.

3.2. Estimated progression of cortical thinning in very early AD

To estimate the progression of regional PHG thinning from aMCI to AD stages, patients' cortical thickness values were transformed into standard (z-) scores based on the mean and standard deviation of their respective demographically matched control group and compared with 2-tailed, unpaired t tests. These analyses revealed that ERC and mPRC significantly differed between aMCI and AD patients, while lPRC and PHC did not [ERC: $t(55) = 2.622$, $p < 0.05$; mPRC: $t(55) = 2.414$, $p < 0.05$; lPRC: $t(55) = 0.750$, $p = 0.456$; PHC: $t(55) = 0.155$, $p = 0.878$; see Fig. 1].

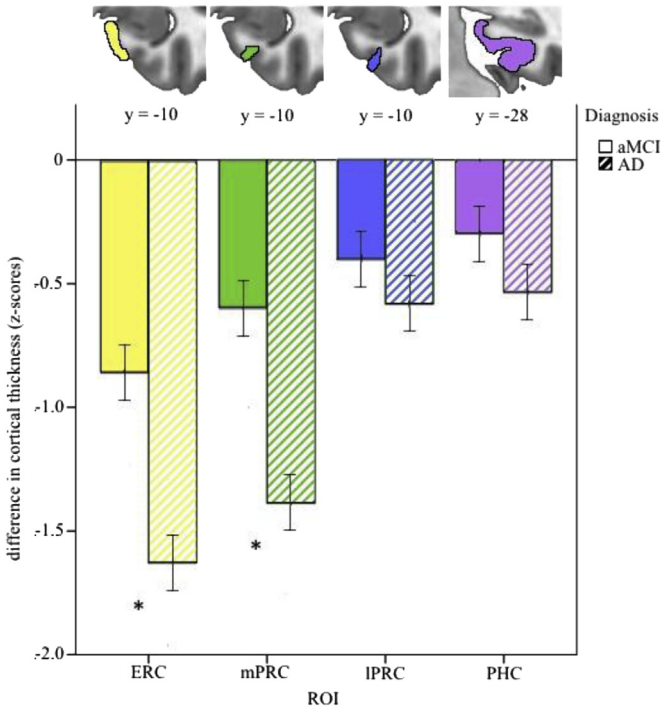

Fig. 1. Z-transformed mean thickness values for aMCI and AD participants for each ROI. Standard error bars are displayed (±1 SE). *Significant differences at $p < 0.05$. Abbreviations: AD, Alzheimer's dementia; aMCI, amnestic mild cognitive impairment; ERC, entorhinal cortex; lPRC, lateral perirhinal cortex; mPRC, medial perirhinal cortex; PHC, parahippocampal cortex; ROI, region of interest; SE, standard error.

3.3. Coronal levels displaying maximal ERC and mPRC thinning in aMCI and AD patients

In the clinical setting, coronal slices of anatomic MRI scans are examined for PHG thinning indicative of AD. The next analysis aimed to determine whether ERC and mPRC thinning was disproportionately manifested in specific coronal (MNI y-coordinate) levels. To address this question, we compared normalized cortical thickness values at each vertex coordinate of the NC versus AD group. This analysis was conducted on y-levels containing minimally 90%–95% of the distribution of data points, corresponding to the mid anterior-to-posterior section (MNI y-levels between −22 and −3), to minimize spurious findings.

Two univariate ANOVAs, one for the mPRC and one for the ERC, with mean normalized cortical thickness values at each y-level as the dependent variable, and diagnosis, hemisphere and MNI y-coordinate as independent variables, were conducted to determine whether cortical thinning (i.e., a difference between control and patient thickness) was exacerbated at specific y-levels (i.e., a significant interaction between group and y-level). This was indeed the case for both the ERC and mPRC: we found a 3-way interaction between group, y-level, and hemisphere [ERC: $F(19, 31{,}765) = 3.241$, $p < 0.001$; mPRC: $F(19, 30{,}533) = 2.703$, $p < 0.001$]. Additional post hoc tests identified the nature of these interactions, that is, that maximal cortical thinning in the ERC and mPRC was constrained to different y-levels in each hemisphere. Specifically, left hemisphere ERC cortical thinning was maximal at y-levels −3 to −5, and in levels −5 to −7 in the right hemisphere (Bonferroni-corrected univariate ANCOVAs of NC vs. AD and left hemisphere y-levels (MNI y-levels between −22 and −3): $F(19, 16{,}221) = 14.866$, $p < 0.0125$; same ANCOVA with right hemisphere y-levels: $F(19, 165541) = 9.705$, $p < 0.0125$). Maximal cortical thickness in the mPRC was also evident at different anterior-to-posterior extents. In the left

Table 4
MNI y-coordinates (coronal levels) maximally differentiating NC from very early AD patients

ROI	NC versus AD	
	Left hemisphere	Right hemisphere
	y-level (ES, SD)	y-level (ES, SD)
ERC	**−3 (1.26, 0.082)**	−5 (1.06, 0.076)
	−4 (1.01, 0.079)	−6 (1.11, 0.074)
	−5 (0.95, 0.082)	−7 (1.08, 0.078)
mPRC	−7 (0.86, 0.060)	**−7 (0.90, 0.067)**
	−8 (1.01, 0.058)	**−8 (0.93, 0.065)**

Bolded text represents vertices of maximal differences in cortical thickness between AD patients and healthy controls.
Key: AD, Alzheimer's dementia; ERC, entorhinal cortex; ES, effect size; mPRC, medial perirhinal cortex; NC, normal controls; ROI, region of interest; SD, standard deviation.

Table 3
Normalized and retransformed mean cortical thicknesses in each ROI over both hemispheres

Group	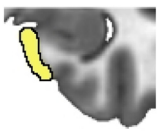	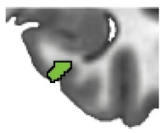	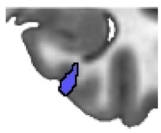	
	y = −10	y = −10	y = −10	y = −28
	ERC	mPRC	lPRC	PHC
	M (SD)	M (SD)	M (SD)	M (SD)
NC versus aMCI				
NC (n = 46)	3.65 (0.29)	2.98 (0.36)	3.24 (0.43)	2.65 (0.31)
aMCI (n = 23)	3.37 (0.37)	2.71 (0.51)	3.08 (0.39)	2.55 (0.26)
Relative difference (%)	8	9	5	4
NC versus AD				
NC (n = 31)	3.61 (0.33)	2.91 (0.35)	3.23 (0.45)	2.61 (0.31)
AD (n = 34)	2.95 (0.44)	2.27 (0.49)	2.90 (0.51)	2.45 (0.34)
Relative difference (%)	18	22	10	6

M and SD, both values are displayed in mm and were transformed as described in Section 2.3.
Key: AD, Alzheimer's dementia; aMCI, amnestic mild cognitive impairment; ERC, entorhinal cortex; lPRC, lateral perirhinal cortex; M, mean; mPRC, medial perirhinal cortex; NC, normal controls; PHC, parahippocampal cortex; ROI, region of interest; SD, standard deviation.

hemisphere, maximal differences in mPRC cortical thickness was found at y = −8, whereas maximal differences in the right hemisphere mPRC was specific to y-levels −7 and −8 [Bonferroni-corrected univariate ANCOVAs of NC vs. AD and left hemisphere y-levels (MNI y-levels between −22 and −3): $F(19, 15{,}769) = 2.590$, $p < 0.0125$; same ANCOVA with right hemisphere y-levels: $F(19, 14{,}761) = 4.195$, $p < 0.0125$]. Table 4 summarizes these results by indicating the MNI y-coordinates where NCs maximally differed from AD patients (i.e., where $p < 0.05$ and effect size ≥0.3). To illustrate the general patterns of atrophy, the distribution of cortical thickness differences between NCs and AD patients in the ERC and mPRC are plotted in Fig. 2. We note that although the maximal difference in NC versus AD ERC cortical thickness was found in the right hemisphere (cf. red portion of ERC difference, Fig. 2), the nature of the variance at each y-level generated the largest statistical difference in the left hemisphere ERC.

4. Discussion

Patients with aMCI evidence cortical thinning of the mPRC as well as the ERC but neither the lPRC nor the PHC. However, the lPRC was also significantly atrophied in AD patients. The cortical thickness of the PHC remained intact in the aMCI and AD patients. With increasing clinical progression at this early stage (aMCI vs. early AD), more impaired patients similarly showed significantly thinner mPRC's and ERC's. However, there were no significant differences with respect to the lPRC or PHC when comparing aMCI versus AD patients. These findings based on rigorous anatomic segmentation add new aspects to the literature on atrophy in AD by showing that when patients in the earliest stages of AD are investigated, differential thinning can indeed be documented within ROIs of the PHG, in contrast to negative results from previous reports (e.g., Dickerson et al., 2009; Teipel et al., 2006). The present findings are relevant to

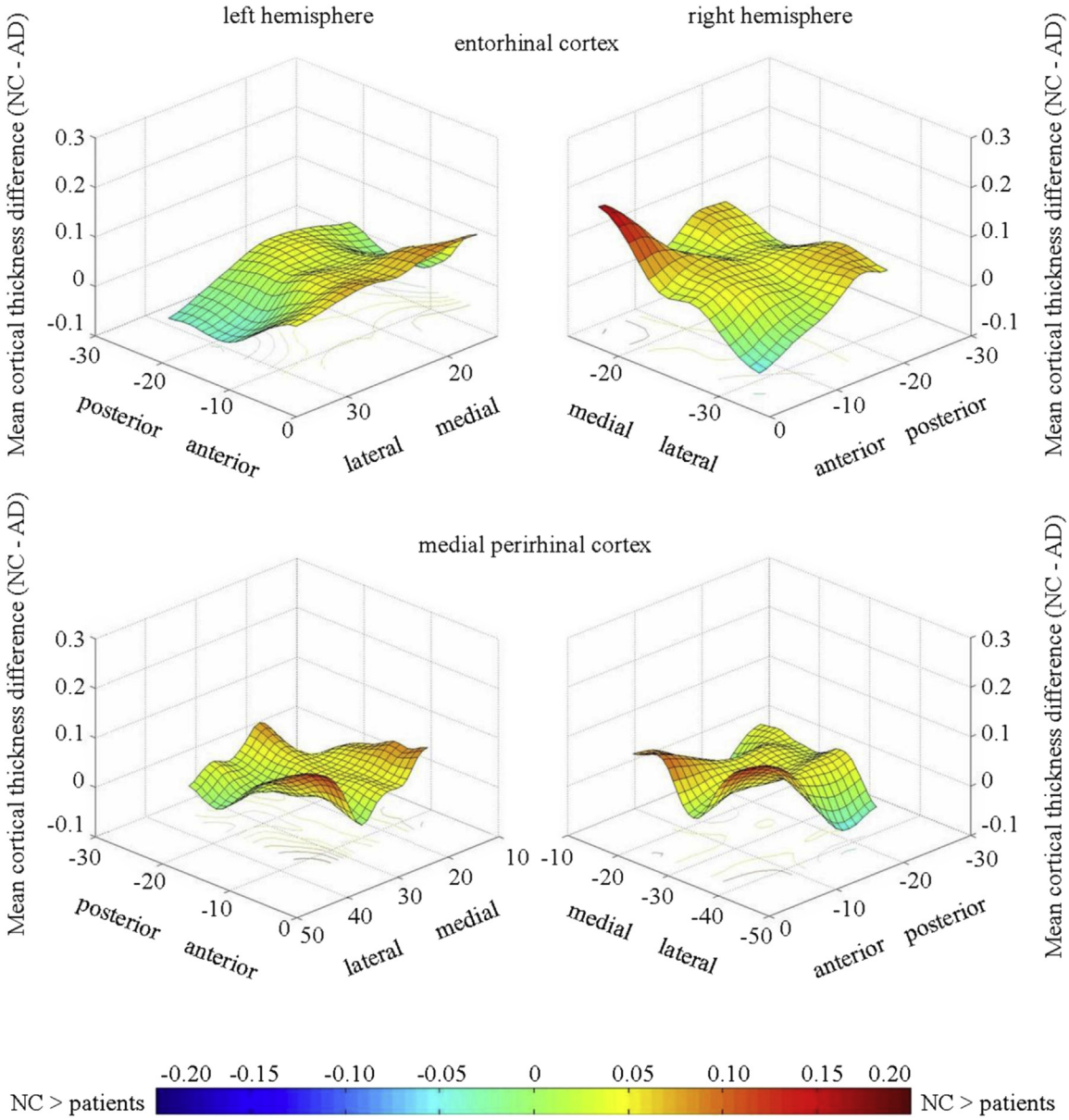

Fig. 2. Differences in mean vertex-wise cortical thickness values between NC and AD participants. Red colors display areas where NCs show higher mean cortical thickness values than patients, blue colors represent the opposite. Abbreviations: AD, Alzheimer's dementia; NC, normal controls.

understanding the relationship between the hierarchical order of cortical progression of NFT pathology and regional cortical thinning, as well as the associated cognitive impairments predicted in the earliest stages of the disease. Finally, the present findings generate recommendations for the reliable and practical clinical identification of early AD-associated thinning on structural MRI scans.

The staging of NFT-related pathology predicts that NFTs occur first in the mPRC followed by the ERC, and much later in the lPRC (Braak and Braak, 1995). This stereotypical pattern of NFT progression is presumed to be accompanied with thinning in the respective regions, although the precise mechanism relating NFT pathology with cortical atrophy (and neuronal functioning) remains to be determined. The present findings are broadly consistent with this hypothesis: both mPRC and ERC demonstrated thinning in both patient groups, whereas lPRC thickness was atrophied in the AD group only, a pattern which is generally consistent with the spread of cortical neurofibrillary pathology as described by Braak and Braak (1991, 1995). However, we found no evidence that the mPRC was atrophied to a greater extent than the ERC, as hypothesized from the anatomic progression of NFT. Similar negative findings were reported by other research groups (Dickerson et al., 2001; Galton et al., 2001; Jack et al., 1997; Kordower et al., 2001; Scahill et al., 2002; Xu et al., 2000), although these studies did not segment the mPRC from the lPRC and investigated patients in more advanced or variable stages of the disease. It seems that the ERC and mPRC may show comparable relative thinning in the early stages of AD. Because the ERC is thicker than the mPRC (e.g., Dickerson et al., 2009), the ERC would show greater absolute change in thickness than the mPRC (e.g., a 10% reduction in a 4-mm cortical thickness is a greater absolute change than a 10% reduction in a 3 mm cortical thickness). However, thinning relative to region size is expected to be comparable in both ROIs or greater in mPRC than ERC in the earliest stages of the atrophy since the former structure is affected first (Braak et al., 1991, 1995). Indeed, we found comparable or slightly greater relative decreases in patients' mPRC (9% and 22% for aMCI and AD patients, respectively) than their ERC (8% and 18% for aMCI and AD patients, respectively). We note that the estimates of relative ERC thinning are comparable to those reported by Velayudhan et al. (2013) using the automatic ERC segmentation tool provided by FreeSurfer (NC vs. MCI: 7%; NC vs. AD: 19%; present study: NC vs. aMCI: 8%; NC vs. AD: 18%). The availability of MRI processing software, which automatically and reliably segments the ERC (Desikan et al., 2006; Fischl et al., 2002; Shaker and Soltanian-Zadeh, 2008; Yushkevich et al., 2015) and recently the mPRC (Augustinack et al., 2013), noticeably economizes the segmentation process compared to manual segmentation. However, the validity of the automatic mPRC segmentation remains to be established, especially for complex (e.g., bifurcated) CS, although very recent effort in this direction has been made (e.g., Yushkevich et al., 2015).

Critically, the present study found no significant PHC thinning in the aMCI and AD groups. This finding contrasts with those reported by Teipel et al. (2006) and Dickerson et al. (2009), both of whom reported significant PHC atrophy in their AD patients. However, the patients investigated in these studies were in more advanced disease stages (mean MMSE score, 23.1 [lowest score, 10], respectively, MMSE range, 16–28) compared to the present samples (MMSE range 22–30). Correspondingly, Thangavel et al. (2008) report substantial NFT load in layers III and V of areas TF (area fusiformis) and TH (area temporohippocampica; corresponding with the PHC) in postmortem brains of AD patients in presumably severe stages of their disease (9–12 years disease duration). Thus, taken together, the results of these and the present studies indicate that atrophy of the mPRC and ERC occurs before atrophy of the PHC. Clearly, individuals in prodromal stages of the disease who are later definitively diagnosed with Alzheimer's disease must be longitudinally studied to determine the first cortical site of atrophy and the longitudinal progression of atrophy in the PHG substructures.

Detailed vertex-vice investigations of cortical thickness values revealed the coronal slices with maximal ERC and mPRC cortical thinning in AD versus control participants, namely anterior slices ranging from MNI y = −3 to −8, that is, the region between 4 and 9 mm posterior to the most anterior slice where the amygdala is first visible. Although for ERC the most discriminative slices were situated in the left hemisphere only, they were situated in both hemispheres for mPRC. These findings can be applied in the clinical setting to reliably detect ERC and mPRC thinning in potential very early AD patients. To our knowledge, this is the first study that provides specific y-MNI coordinates that aim to support the process of AD diagnosis in the clinical as well as the research setting.

The cognitive domains that appear to be affected in the earliest stages of aMCI and AD using standard clinical neuropsychological tests are verbal and visual episodic memory (Salmon, 2011). Indeed, a recent study by Mistridis et al. (2015) demonstrates that verbal memory performance declined already 8 years before the diagnosis of MCI preceding AD (n = 27) compared to 60 participants who remained cognitively healthy. These neurocognitive functions are strongly associated with the hippocampus and the ERC (Lipton and Eichenbaum, 2008). The PRC, which is affected by NFT before the ERC, has been associated with the processing of semantic object memories and object recognition memory (Kivisaari et al., 2013b). Although some studies report that these functions, when measured by the semantic fluency test, decline first or concurrently with episodic memory (Amieva et al., 2005, 2008), most studies report that decline in episodic memory precedes semantic memory impairment (Grober et al., 2008; Saxton et al., 2004). However, common clinical tests of semantic memory, such as semantic fluency, may not be sensitive enough to specific kinds of disturbances in semantic object processing associated with PRC dysfunction that have been described in recent years (see e.g., Hirni et al., 2013; Kivisaari et al., 2012, 2013a; Moss et al., 2005; Tyler et al., 2004). More specific cognitive tasks based on cognitive neuroscience models of PRC functioning should be developed to take advantage of the progress made in this domain and translate it to the clinical research setting. Therefore, measures of cortical thickness can be applied most effectively as part of comprehensive multimodal diagnostic assessment for AD including advanced neuropsychological testing and where possible PET and/or MR functional imaging.

The present results demonstrate that the mPRC and ERC are atrophied in very early AD, whereas the thickness of the PHC remains within normal limits. The lPRC was significantly atrophied in the AD, but not in the aMCI group. Studies investigating more advanced AD patients demonstrate that all PHG substructures—the PRC, ERC, and PHC—are comparably atrophic. Thus, the present findings regarding mPRC and ERC thinning broadly map onto the hierarchical progression of neurofibrillary pathology described by Braak and Braak (1991, 1995). Critically, they further suggest that cognitive impairments associated with the PHC (e.g., dysfunctional processing of visuospatial and landmark information) are still not present in the earliest stages of the AD, whereas those related to the mPRC and ERC represent promising cognitive markers of incipient AD.

Disclosure statement

The authors have nothing to disclose.

Acknowledgements

This study was supported by grants from the Swiss National Science Foundation (Ambizione fellowship PZ00P1_126493 [Kirsten I Taylor] and grant 3200-049107 [Andreas U Monsch]), the Alfred and Anneliese Sutter-Stöttner Stiftung (Andreas U Monsch), and Novartis Foundations, Basel (Andreas U Monsch), Switzerland.

References

American Psychichiatric Association, 1994. Diagnostic and Statistical Manual of Mental Disorders. American Psychiatric Press, Washington DC.

Amieva, H., Jacqmin-Gadda, H., Orgogozo, J.-M., Le Carret, N., Helmer, C., Letenneur, L., Barberger-Gateau, P., Fabrigoule, C., Dartigues, J.F., 2005. The 9 year cognitive decline before dementia of the Alzheimer type: a prospective population-based study. Brain J. Neurol. 128, 1093–1101.

Amieva, H., Le Goff, M., Millet, X., Orgogozo, J.-M., Pérès, K., Barberger-Gateau, P., Jacqmin-Gadda, H., Dartigues, J.F., 2008. Prodromal Alzheimer's disease: successive emergence of the clinical symptoms. Ann. Neurol. 64, 492–498.

Augustinack, J.C., Huber, K.E., Stevens, A.A., Roy, M., Frosch, M.P., van der Kouwe, A.J., Wald, L.L., Van Leemput, K., McKee, A.C., Fischl, B., Alzheimer's Disease Neuroimaging Initiative, 2013. Predicting the location of human perirhinal cortex, Brodmann's area 35, from MRI. Neuroimage 64, 32–42.

Ball, M.J., 1978. Topographic distribution of neurofibrillary tangles and granulovacuolar degeneration in hippocampal cortex of aging and demented patients. A quantitative study. Acta Neuropathol. 42, 73–80.

Braak, H., Braak, E., 1985. On areas of transition between entorhinal allocortex and temporal isocortex in the human brain. Normal morphology and lamina-specific pathology in Alzheimer's disease. Acta Neuropathol. 68, 325–332.

Braak, H., Braak, E., 1991. Neuropathological stageing of Alzheimer-related changes. Acta Neuropathol. 82, 239–259.

Braak, H., Braak, E., 1995. Staging of Alzheimer's disease-related neurofibrillary changes. Neurobiol. Aging 16, 271–284.

Braak, H., Del Tredici, K., 2006. Staging of cortical neurofibrillary inclusions of the Alzheimer's type. In: Jucker, M., Beyreuther, K., Haass, C., Nitsch, R.M., Christen, Y. (Eds.), Alzheimer: 100 Years and beyond. Springer; Berlin Heidelberg, pp. 97–106.

Critchley, M., 1953. The parietal lobes, vii. Williams and Wilkins, Oxford, England.

Dale, A.M., Fischl, B., Sereno, M.I., 1999. Cortical surface-based analysis. I. Segmentation and surface reconstruction. Neuroimage 9, 179–194.

Delis, D.C., Kramer, J.H., Kaplan, E., Ober, B.A., 1987. California Verbal Learning Test. Psychological Corporation, San Antonio, Texas.

Desikan, R.S., Ségonne, F., Fischl, B., Quinn, B.T., Dickerson, B.C., Blacker, D., Buckner, R.L., Dale, A.M., Maguire, R.P., Hyman, B.T., Albert, M.S., Killiany, R.J., 2006. An automated labeling system for subdividing the human cerebral cortex on MRI scans into gyral based regions of interest. Neuroimage 31, 968–980.

Dickerson, B.C., Feczko, E., Augustinack, J., Pacheco, J., Morris, J., Fischl, B., Buckner, R., 2009. Differential effects of aging and Alzheimer's disease on medial temporal lobe cortical thickness and surface area. Neurobiol. Aging 30, 432–440.

Dickerson, B.C., Sullivan, M.P., Forchetti, C., Wilson, R.S., Bennett, D.A., Beckett, L.A., deToledo-Morrell, L., 2001. MRI-derived entorhinal and hippocampal atrophy in incipient and very mild Alzheimer's disease. Neurobiol. Aging 22, 747–754.

Du, A.T., Schuff, N., Amend, D., Laakso, M.P., Hsu, Y.Y., Jagust, W.J., Yaffe, K., Kramer, J.H., Reed, R., Norman, D., Chui, H.C., Weiner, M.W., 2001. Magnetic resonance imaging of the entorhinal cortex and hippocampus in mild cognitive impairment and Alzheimer's disease. J. Neurol. Neurosurg. Psychiatry 71, 441–447.

Epstein, R., Kanwisher, N., 1998. A cortical representation of the local visual environment. Nature 392, 598–601.

Fischl, B., Dale, A.M., 2000. Measuring the thickness of the human cerebral cortex from magnetic resonance images. Proc. Natl. Acad. Sci. U. S. A. 97, 11050–11055.

Fischl, B., Salat, D.H., Busa, E., Albert, M., Dieterich, M., Haselgrove, C., van der Kouwe, A., Killiany, R., Kennedy, D., Klaveness, S., Montillo, A., Makris, N., Rosen, B., Dale, A.M., 2002. Whole brain segmentation: automated labeling of neuroanatomical structures in the human brain. Neuron 33, 341–355.

Folstein, M.F., Folstein, S.E., McHugh, P.R., 1975. "Mini Mental State"—a practical method for grading the cognitive state of patients for the clinician. J. Psychiatry Res. 12, 189–198.

Galton, C.J., Patterson, K., Graham, K., Lambon, R., Williams, G., Antoun, N., Sahakian, B.J., Hodges, J.R., 2001. Differing patterns of temporal atrophy in Alzheimer's disease and semantic dementia. Neurology 57, 216–225.

Geddes, J.W., Tekirian, T.L., Soultanian, N.S., Ashford, J.W., Davis, D.G., Markesbery, W.R., 1997. Comparison of neuropathologic criteria for the diagnosis of Alzheimer's disease. Neurobiol. Aging 18 (4, Supplement 1), 99–105.

Gómez-Isla, T., Hollister, R., West, H., Mui, S., Growdon, J.H., Petersen, R.C., Parisi, J.E., Hyman, B.T., 1997. Neuronal loss correlates with but exceeds neurofibrillary tangles in Alzheimer's disease. Ann. Neurol. 41, 17–24.

Grober, E., Hall, C.B., Lipton, R.B., Zonderman, A.B., Resnick, S.M., Kawas, C., 2008. Memory impairment, executive dysfunction, and intellectual decline in preclinical Alzheimer's disease. J. Int. Neuropsychol. Soc. 14, 266–278.

Hanke, J., 1997. Sulcal pattern of the anterior parahippocampal gyrus in the human adult. Ann. Anat. 179, 335–339.

Hirni, D.I., Monsch, A.U., Kivisaari, S.L., Reinhardt, J., Ulmer, S., Stippich, C., Taylor, K.I., 2013. Impaired medial perirhinal cortex functioning twelve years preceding diagnosis of Alzheimer's disease. Poster Present Annu Meet Soc Neurosci, San Diego, USA.

Im, K., Lee, J.M., Seo, S.W., Hyung Kim, S., Kim, S.I., Na, D.L., 2008. Sulcal morphology changes and their relationship with cortical thickness and gyral white matter volume in mild cognitive impairment and Alzheimer's disease. Neuroimage 43, 103–113.

Insausti, R., Juottonen, K., Soininen, H., Insausti, A.M., Partanen, K., Vainio, P., Laakso, M.P., Pitkänen, A., 1998. MR volumetric analysis of the human entorhinal, perirhinal, and temporopolar cortices. Am. J. Neuroradiol. 19, 659–671.

Jack, C.R., Petersen, R.C., Xu, Y.C., Waring, S.C., O'Brien, P.C., Tangalos, E.G., Smith, G.E., Ivnik, R.J., Kokmen, E., 1997. Medial temporal atrophy on MRI in normal aging and very mild Alzheimer's disease. Neurology 49, 786–794.

Juottonen, K., Laakso, M.P., Insausti, R., Lehtovirta, M., Pitkänen, A., Partanen, K., Soininen, H., 1998. Volumes of the entorhinal and perirhinal cortices in Alzheimer's disease. Neurobiol. Aging 19, 15–22.

Kaplan, E., Goodglass, H., Weintraub, S., Goodglass, H., 1983. Boston naming Test. Lea & Febiger, Philadelphia.

Kivisaari, S.L., Monsch, A.U., Taylor, K.I., 2013a. False positives to confusable objects predict medial temporal lobe atrophy. Hippocampus 9, 832–841.

Kivisaari, S.L., Probst, A., Taylor, K.I., 2013b. The perirhinal, entorhinal and parahippocampal cortices and hippocampus: an overview of functional anatomy and protocol for their segmentation in MR images. In: Ulmer, S., Jansen, O. (Eds.), fMRI: Basics and Clinical Application. Springer, Berlin, pp. 239–304.

Kivisaari, S.L., Tyler, L.K., Monsch, A.U., Taylor, K.I., 2012. Medial perirhinal cortex disambiguates confusable objects. Brain 135, 3757–3769.

Kordower, J.H., Chu, Y., Stebbins, G.T., DeKosky, S.T., Cochran, E.J., Bennett, D., Mufson, E.J., 2001. Loss and atrophy of layer II entorhinal cortex neurons in elderly people with mild cognitive impairment. Ann. Neurol. 49, 202–213.

Lerch, J.P., Pruessner, J.C., Zijdenbos, A., Hampel, H., Teipel, S.J., Evans, A.C., 2005. Focal decline of cortical thickness in Alzheimer's disease identified by computational neuroanatomy. Cereb. Cortex 15, 995–1001.

Lipton, P.A., Eichenbaum, H., 2008. Complementary roles of hippocampus and medial entorhinal cortex in episodic memory. Neural Plast. 2008, 258467.

Mistridis, P., Krumm, S., Monsch, A.U., Berres, M., Taylor, K.I., 2015. The 12 years preceding mild cognitive impairment due to Alzheimer's disease: The temporal emergence of cognitive decline. J. Alzheimers Dis. 48, 1095–1107.

Moss, H.E., Rodd, J.M., Stamatakis, E.A., Bright, P., Tyler, L.K., 2005. Anteromedial temporal cortex supports fine-grained differentiation among objects. Cereb. Cortex 15, 616–627.

Nelson, P.T., Alafuzoff, I., Bigio, E.H., Bouras, C., Braak, H., Cairns, N.J., Castellani, R.J., Crain, B.J., Davies, P., Del Tredici, K., Duyckaerts, C., Frosch, M.P., Haroutunian, V., Hof, P.R., Hulette, C.M., Hyman, B.T., Iwatsubo, T., Jellinger, K.A., Jicha, G.A., Kövari, E., Kukull, W.A., Leverenz, J.A., Love, S., Mackenzie, I.R., Mann, D.M., Masliah, E., McKee, A.C., Montine, T.J., Morris, J.C., Schneider, J.A., Sonnen, J.A., Thal, D.R., Trojanowski, J.Q., Troncoso, J.C., Wisniewski, T., Woltjer, R.L., Beach, T.G., 2012. Correlation of Alzheimer disease neuropathologic changes with cognitive status: a review of the literature. J. Neuropathol. Exp. Neurol. 71, 362–381.

Petersen, R.C., Parisi, J.E., Dickson, D.W., Johnson, K.A., Knopman, D.S., Boeve, B.F., Jicha, G.A., Ivnik, R.J., Smith, G.E., Tangalos, E.G., Braak, H., Kokmen, E., 2006. Neuropathologic features of amnestic mild cognitive impairment. Arch. Neurol. 63, 665–672.

Pruessner, J.C., Köhler, S., Crane, J., Pruessner, M., Lord, C., Byrne, A., Kabani, N., Collins, D.L., Evans, A.C., 2002. Volumetry of the temporopolar, perirhinal, entorhinal and parahippocampal cortex from high-resolution MRI images: considering the variability of the collateral sulcus. Cereb. Cortex 12, 1342–1353.

Salmon, D.P., 2011. Neuropsychological features of mild cognitive impairment and preclinical Alzheimer's disease. Curr. Top Behav. Neurosci. 10, 187–212.

Saxton, J., Lopez, O.L., Ratcliff, G., Dulberg, C., Fried, L.P., Carlson, M.C., Newman, A.B., Kuller, L., 2004. Preclinical Alzheimer disease: neuropsychological test performance 1.5 to 8 years prior to onset. Neurology 63, 2341–2347.

Scahill, R.I., Schott, J.M., Stevens, J.M., Rossor, M.N., Fox, N.C., 2002. Mapping the evolution of regional atrophy in Alzheimer's disease: unbiased analysis of fluid-registered serial MRI. Proc. Natl. Acad. Sci. U. S. A. 99, 4703–4707.

Seo, S.W., Im, K., Lee, J.-M., Kim, S.T., Ahn, H.J., Go, S.M., Kim, S.-H., Na, D.L., 2011. Effects of demographic factors on cortical thickness in Alzheimer's disease. Neurobiol. Aging 32, 200–209.

Shaker, M., Soltanian-Zadeh, H., Automatic segmentation of brain structures from MRI integrating atlas-based labeling and level set method. In: Canadian Conference on Electrical and Computer Engineering. CCECE 2008; 2008. p. 1755–1758.

Skullerud, K., 1984. Variations in the size of the human brain. Influence of age, sex, body length, body mass index, alcoholism, Alzheimer changes, and cerebral atherosclerosis. Acta Neurol. Scand. Suppl. 102, 1–94.

Taylor, K.I., Probst, A., 2008. Anatomic localization of the transentorhinal region of the perirhinal cortex. Neurobiol. Aging 29, 1591–1596.

Teipel, S.J., Pruessner, J.C., Faltraco, F., Born, C., Rocha-Unold, M., Evans, A., Möller, H.-J., Hampel, H., 2006. Comprehensive dissection of the medial temporal lobe in AD: measurement of hippocampus, amygdala, entorhinal, perirhinal and parahippocampal cortices using MRI. J. Neurol. 253, 794–800.

Thangavel, R., van Hoesen, G.W., Zaheer, A., 2008. Posterior parahippocampal gyrus pathology in Alzheimer's disease. Neuroscience 154, 667–676.

Tyler, L.K., Stamatakis, E.A., Bright, P., Acres, K., Abdallah, S., Rodd, J.M., Moss, H.E., 2004. Processing objects at different levels of specificity. J. Cogn. Neurosci. 16, 351–362.

Van Hoesen, G.W., Augustinack, J.C., Dierking, J., Redman, S.J., Thangavel, R., 2000. The parahippocampal gyrus in Alzheimer's disease: clinical and preclinical neuroanatomical correlates. Ann. N. Y. Acad. Sci. 911, 254–274.

Velayudhan, L., Proitsi, P., Westman, E., Muehlboeck, J.-S., Mecocci, P., Vellas, B., Tsolaki, M., Kłoszewska, I., Soininen, H., Spenger, C., Hodges, A., Powell, J., Lovestone, S., Simmons, A., 2013. Entorhinal cortex thickness predicts cognitive decline in Alzheimer's disease. J. Alzheimers Dis. 33, 755–766.

Winblad, B., Palmer, K., Kivipelto, M., Jelic, V., Fratiglioni, L., Wahlund, L.-O., Nordberg, A., Bäckman, L., Albert, M., Almkvist, O., Arai, H., Basun, H., Blennow, K., De Leon, M., Decarli, C., Erkinjuntti, T., Giacobini, E., Graff, C., Hardy, J., Jack, C., Jorm, A., Ritchie, K., Van Duijn, C., Visser, P., Petersen, R.C., 2004. Mild cognitive impairment—beyond controversies, toward a consensus: report of the International Working Group on Mild Cognitive Impairment. J. Intern. Med. 256, 240–246.

Xu, Y., Jack, C.R., O'Brien, P.C., Kokmen, E., Smith, G.E., Ivnik, R.J., Boeve, B.F., Tangalos, R.G., Petersen, R.C., 2000. Usefulness of MRI measures of entorhinal cortex versus hippocampus in AD. Neurology 54, 1760–1767.

Yushkevich, P.A., Pluta, J.B., Wang, H., Xie, L., Ding, S.-L., Gertje, E.C., Mancuso, L., Kliot, D., Das, S.R., Wolk, D.A., 2015. Automated volumetry and regional thickness analysis of hippocampal subfields and medial temporal cortical structures in mild cognitive impairment. Hum. Brain Mapp. 36, 258–287.